

Reactions of Nitromethane on Si(100): First-Principles Predictions

José A. Barriocanal and D. J. Doren*

Department of Chemistry, University of Delaware, Newark, Delaware 19716

Received: June 16, 2000; In Final Form: October 26, 2000

Reactions of nitromethane on Si(100) are investigated using density functional theory. Calculations show that nitromethane should strongly chemisorb to the surface dimer by means of a 1,3-dipolar cycloaddition reaction pathway, with no significant activation barrier. Though the 1,3-dipolar cycloaddition results in a strongly bound product, this initial cycloadduct is metastable with respect to rearrangement products formed through oxygen migrations between lattice silicons. Multiple products are likely to be present on the surface, so that it will not be well ordered. This reaction suggests a new route for attaching organic monolayers to Si(100) and provides a model system for bonding in silicon oxynitride films.

I. Introduction

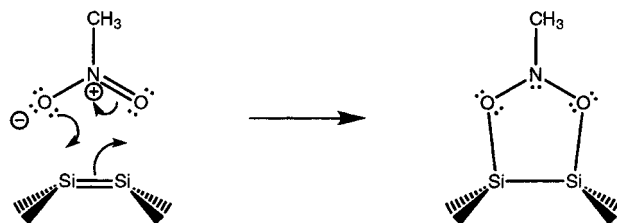
There has been a great deal of recent work on chemical approaches to forming covalently bound organic monolayers on silicon surfaces. In addition to its fundamental interest as novel chemistry, this effort is driven by potential applications in areas such as nonlinear optical materials, lithography, interfaces between Si and organic optoelectronic materials, sensors, DNA chips, molecular electronics, and nanomachine lubricants.

Here we describe theoretical studies of a new class of reactions between organic molecules and the Si(100)-2×1 surface. These reactions are the surface analogues of reactions from organic synthesis, known as 1,3-dipolar additions.¹ This paper explores a prototypical example, the nondissociative chemisorption of nitromethane to form a ring structure, as indicated in Scheme 1.

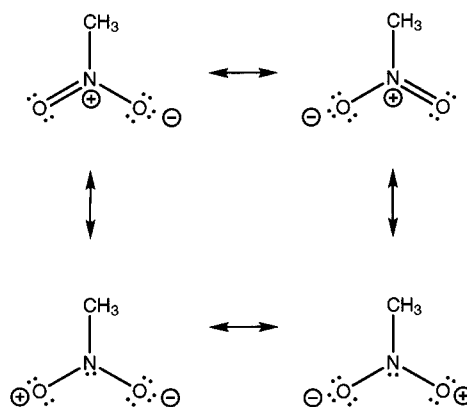
We have denoted the surface dimer bond as a π -bond, to emphasize the analogy with the corresponding reaction of C–C π -bonds. Of course, the interaction between dimer dangling bonds is quite weak, amounting to less than 10 kcal/mol,^{2–7} so that the dimer will be much more reactive than a C–C π -bond or even a molecular Si–Si π -bond. The arrows in Scheme 1 indicate formal rearrangement of electron pairs; the charges shown are discussed below. This reaction can be described as a [4+2] cycloaddition, in which nitromethane formally contributes four π -electrons while the surface dimer contributes two π -electrons. Nitromethane is known as a 1,3-dipole because of the sextet resonance structure shown in Scheme 2.

These resonance structures do not indicate anything about the actual charge distribution in nitromethane (note that the mirror images of the structures shown must contribute equally to the electron distribution of the isolated molecule), but reflect the high polarizability of the molecule. A large class of other molecules also have this 1,3-dipolar character, including nitroalkanes (R–NO₂), azides (R–NNN), nitrileoxides (R–CNO), and diazo compounds (R–CNN). All of these molecules can react by the same formal mechanism shown for nitromethane, as can analogous reagents with sulfur replacing oxygen or phosphorus replacing nitrogen. The organic group, R, has little influence on reactivity (as long as it contains no other functional

SCHEME 1



SCHEME 2



groups that can react with the surface) and can be chosen as needed for particular applications. If this class of reactions runs efficiently on the Si(100) surface, the wide variety of possible reagents (with various choices for both R and the functional group) will allow new opportunities for controlling properties of the adsorbate layers.

There are good qualitative reasons to expect 1,3-dipolar addition to proceed on Si(100)-2×1 with little or no activation barrier. Previous work has shown that the surface dimer reacts readily in [4+2] cycloadditions with conjugated dienes (the so-called Diels–Alder reaction).^{8,9} The surface reactivity in this case is consistent with that expected for a very reactive π -bond, having little or no activation barrier. However, in contrast to a typical C–C π bond, the lowest energy Si(100) dimer structure is asymmetric (see refs 10 and 11 for a recent review of the evidence) due to a second-order Peierls distortion.¹² In this asymmetric structure one dimer atom is more electron rich than

* Corresponding author. E-mail: doren@udel.edu.

the other, giving the bond a dipolar character. Similar asymmetric dimers are a common feature of transition state structures in dissociative chemisorption of small hydrides.^{10,13–16} Even for [4+2] cycloaddition of a conjugated diene, which is not forbidden from following a symmetric reaction path, theoretical predictions show that the lowest energy reaction path is asymmetric.⁸ Thus, the Si(100) surface appears to react preferentially via asymmetric pathways, in which the surface dimer has dipolar character. A 1,3-dipolar molecule, being easily polarizable, should be able to respond in a complementary way to the presence of the surface dipole, polarizing to allow an electron-rich (poor) oxygen of the molecule to react with the electron-poor (rich) atom of a surface dimer (Scheme 1). This may even allow electrostatic steering toward favorable geometries for reaction.

We have used first-principles theoretical methods, described in section II, to study the chemisorption of nitromethane on the Si(100)-2×1 surface. The predicted reaction energetics and mechanisms are described in section IIIA. However, the initial product of nitromethane adsorption is energetically unstable with respect to products of some subsequent rearrangement reactions (isomers). The relative energetics of several possible rearrangements of the initial nitromethane cycloadduct are discussed in section IIIB. The cycloaddition of other 1,3-dipoles to the Si(100) surface and their subsequent rearrangements are discussed elsewhere.

II. Methods and Models

All calculations described here are based on density functional theory (DFT) using the B3LYP hybrid nonlocal density functional.^{17,18} The Gaussian suite of programs was used to perform the calculations.¹⁹ There are a number of precedents that support the accuracy of this DFT method. The B3LYP functional was used to predict that the reaction barrier for the Diels–Alder reaction on the Si(100) surface is negligible.⁸ These predictions have been confirmed by good agreement with experimental results⁹ and well-correlated wave function calculations.²⁰ Similar calculations of cycloaddition reaction barriers on diamond(100) and Ge(100) also agree well with experiment.^{21,22} Several recent theoretical investigations of Diels–Alder and 1,3-dipolar cycloadditions to the molecular C=C bond have shown that B3LYP predicts transition state and product energetics which are consistent with experiment and higher levels of theory.^{23–28}

For this study, geometries were optimized using a split-valence 6-31G(d) basis set. The Hessian was calculated at each optimized geometry to confirm that it corresponded to a minimum on the potential energy surface. Single-point energies at these optimized geometries were calculated with a larger basis set, 6-311++G(2df,2p). An intermediate basis, 6-311+G(d), was used to explore reaction pathways. All reported energies were calculated with spin-restricted wave functions. In our exploration of the reaction path, wave function stability was confirmed by explicit tests in the initial steps where bonds were not yet fully formed.

The surface model is a Si₉H₁₂ cluster consisting of a single bare surface dimer and subsurface silicons terminated by hydrogens. For adsorption reactions this cluster model gives energetic and geometric predictions in good agreement with experiment and other theoretical methods at reasonable computational cost, though it neglects interactions with adjacent dimers. Some rearrangement products of the initially formed adduct have oxygen atoms inserted into Si–Si bonds. Because such insertions are likely to distort an unconstrained cluster

model in ways that do not realistically reflect surface distortions, constraints were placed on the cluster model geometry in all calculations except those used to explore the initial chemisorption reaction path. Taking the optimized geometry of a C_{2v} symmetric Si₉H₁₂ cluster as a template of an undisturbed lattice, all terminating subsurface hydrogens and the silicons of the third and fourth layers were fixed in their positions. No constraints were imposed on the silicons of the dimer or second layer. These constraints are similar, but not identical, to those used by Stefanov et al. in their studies of surface oxidation.²⁹

In one case, adsorption is considered on a two-dimer model, Si₁₅H₂₁. Constraints were again enforced on the subsurface H atoms and the third and fourth layer Si atoms.

III. Results and Discussion

A. Products of Chemisorption. The [4+2] pericyclic addition of nitromethane to a silicon dimer yields a five-membered ring species as the initial product (Scheme 1 and Figure 1, I). This cycloaddition product is attached to the surface via two coplanar Si–O bonds, with a calculated binding energy of –71.9 kcal/mol (relative to that of the separated nitromethane and surface cluster model). The nitrogen is bent out of the plane of the Si–O bonds, as expected for sp³ hybridization. The methyl group stands normal to the surface. All bond lengths are typical of analogous bonds in molecules.³⁰

An alternative four-membered cycloadduct formed via Si–N and Si–O bonds was also considered (Scheme 3). However, optimization from an initial guess at this structure led directly back to the five-membered ring cycloadduct, indicating that this alternative structure is not stable. An analogous four-membered ring has been considered and has also been excluded as a possible structure on disilenes.³¹

We have also considered the possibility of an adsorption product that bridges across two dimers in the same row (Figure 2). Optimizations done with a two-dimer cluster model yield a binding energy of –45.1 kcal/mol. This is substantially less stable than the single-dimer adsorption product, primarily due to the strain induced by bridging the long distance (3.85 Å) between dimers.

B. Cycloaddition Mechanism. We have investigated the reaction mechanism for nitromethane on Si(100), exploring both symmetric (in which the two Si–O bonds form simultaneously) and asymmetric reaction paths on a single dimer model. We have found no evidence for an activation barrier between the separated reactants and the chemisorbed product on either type of path. Instead, the product was reached on symmetric and asymmetric reaction paths by simply minimizing the energy from an initial geometry with nitromethane and the silicon cluster separated by a large distance. To establish this initial geometry, the relative positions of the molecule and surface cluster were partially optimized while holding the Si–O distance fixed at 2.71 Å (for the asymmetric path, only the shortest Si–O distance was fixed). This distance was chosen to be 1.0 Å longer than the typical Si–O bond length, a value large enough to prevent significant chemical interaction. The geometry found in this partial optimization showed negligible distortion from that of the isolated reactants, and there was minimal interaction between the two reactants in this geometry (counterpoise-corrected energy, relative to the sum of the isolated reactant energies, of –2.31 kcal/mol for the initial symmetric structure; +0.47 kcal/mol for the initial asymmetric structure). Following this partial optimization, the constraint was removed and the energy was minimized. To follow the symmetric path, a C_s

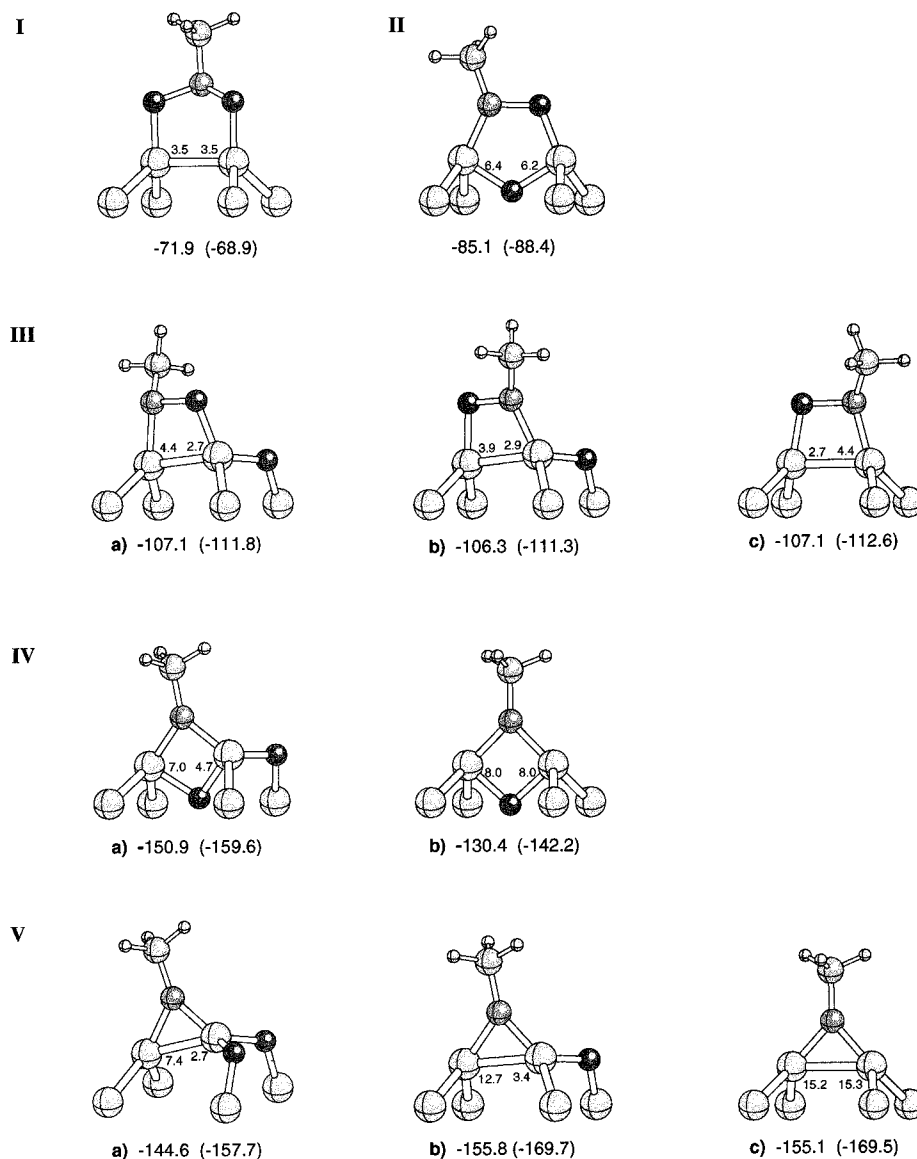
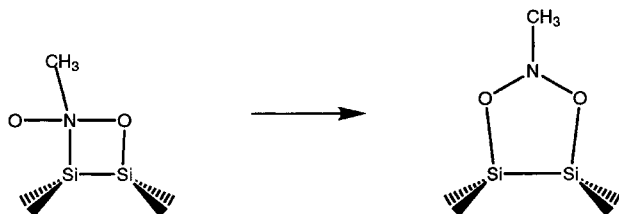


Figure 1. Nitromethane cycloadduct (I) and rearrangement structures (II–V). Energies listed under each figure, in kcal/mol, are with respect to isolated reactants. Energies and geometries are calculated at the B3LYP/6-31G(d) level, with 6-311++G(2df,2p) single-point energies in parentheses. Energies of structures with one or two absent oxygens are calculated, respectively, using the energy of structures b and e in Figure 4. Values of n corresponding to sp^n hybrids are labeled along dimer or Si–O bonds.

SCHEME 3



symmetry plane (bisecting the dimer and including the C–N bond) was imposed throughout the calculation. The asymmetric path was initiated from a geometry in which nitromethane is oriented with one of the oxygens pointing away from the surface (Figure 3). On both paths, the initial geometry is the highest-energy point encountered and minimization proceeds directly to the cycloaddition product. Both of these mechanisms are concerted, in the sense that after a critical configuration has been reached, there is a path to products along which the energy decreases monotonically, without going through any chemically distinct local minima (though we have found other paths that

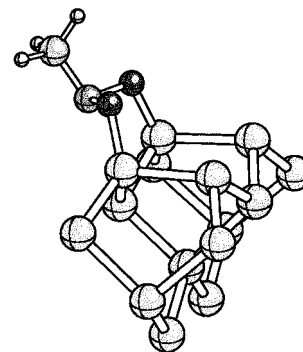


Figure 2. An alternative cycloadduct that bridges two dimers. The binding energy with respect to the isolated reactants is -45.1 kcal/mol at the B3LYP/6-31G(d) level.

pass through local minima corresponding to conformers of the final product).

These calculations imply that there is no significant activation barrier to the chemisorption of nitromethane within a single dimer model. Thus, nitromethane should have a high sticking

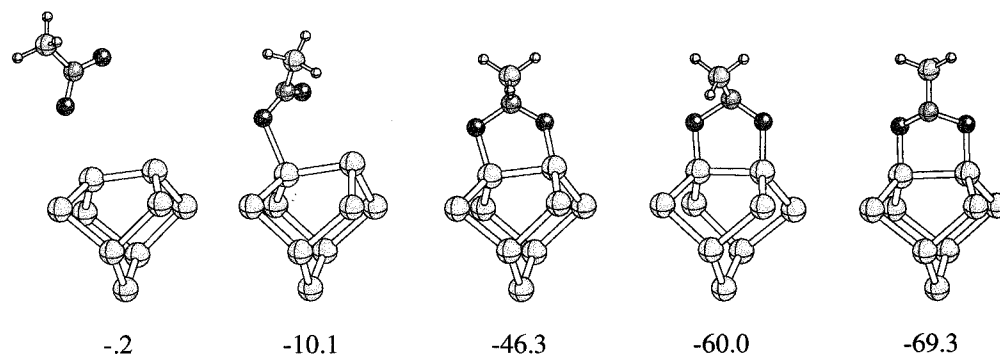


Figure 3. A series of geometries on the reaction path for 1,3-dipolar addition of nitromethane, with energies calculated at the B3LYP/6-311+G(d) level, in kcal/mol relative to the isolated reactants. The counterpoise-corrected interaction energy at the initial geometry is +0.47 kcal/mol.

probability on the Si(100) surface. We have not considered reaction paths that involve multiple dimers, leading to products such as that in Figure 2. However, the unactivated single dimer path of Figure 3 is initiated by a single Si–O interaction, and it is reasonable to expect that the bridging product could form by a similar unactivated path which differs only in that the second Si–O bond is formed with an adjacent dimer. For either product, it is possible that interactions between the adsorbing molecule and adjacent dimers (e.g., steric repulsion between the dimer π -bond and the molecule's methyl group) could alter the reaction path. At higher coverage, interactions with previously adsorbed molecules may also affect the reaction path and activation barrier.

Our calculations predict that the cycloaddition reaction will follow a concerted path, with no evidence of an alternative stepwise mechanism. The question of whether the mechanism of the analogous reaction on C=C double bonds is stepwise or concerted has been the subject of a long controversy.³² However, the experimental evidence indicates that most 1,3-dipolar additions to C=C double bonds follow a concerted path, and current first-principles calculations are in agreement with this picture.^{23–28} Thus, the surface and organic reactions both appear to occur by concerted mechanisms. On the other hand, while organic 1,3-dipolar additions typically have activation energies²⁶ of 10–20 kcal/mol, we find that the surface reaction is unactivated. There are several reasons for this difference. First, the Si dimer π -bond is much weaker than a C–C π -bond, so that there is little energy cost to overcome before the surface can form a bond to the incoming molecule. Second, the initial stage of this reaction involves formation of a Si–O bond. Since Si–O bond energies³³ (108 kcal/mol) are much stronger than those of C–O bonds³³ (86 kcal/mol), the formation of this nascent bond should lower the barrier for the surface reaction more effectively than in the organic analogue. Partial formation of a Si–O bond has also been identified as a stabilizing effect in the transition state for the dissociative adsorption of water.¹⁰

C. Rearrangements. Though the 1,3-dipolar cycloaddition results in a strongly bound cycloadduct, it is metastable with respect to several rearrangement products involving oxygen migration into neighboring Si–Si bonds. Inserting oxygen into a Si–Si bond creates an additional Si–O bond, at the cost of a less favorable N–O bond. Oxygens may migrate from the initially formed five-member ring to the dimer and back-bonds immediately adjacent to the cycloadduct or, at low surface coverages, to neighboring dimers and their back-bonds.

Some of the rearrangement products considered are shown in Figure 1. Rearrangements from the initial 1,3-dipolar cycloadduct, **I**, are organized according to similarity in adsorbate structure. Energies (in kcal/mol) relative to separated reactants calculated with the 6-31G(d) basis and the 6-311++G(2df,2p)

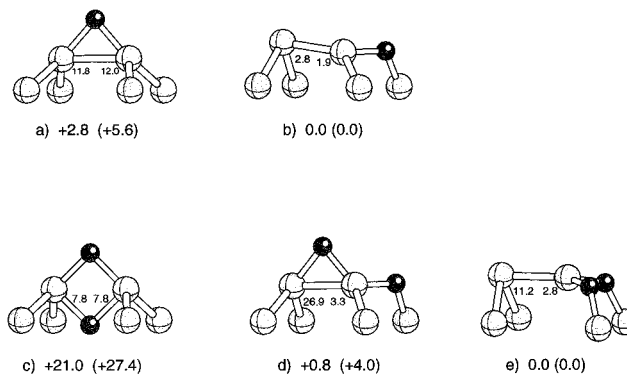


Figure 4. Structures resulting from oxygen migration to neighboring dimers and back-bonds. Energies listed below each structure, in kcal/mol, are with respect to the most stable structure with the corresponding number of oxygens. Energies and geometries are calculated at the B3LYP/6-31G(d) level, with 6-311++G(2df,2p) single point energies in parentheses. Values of n corresponding to sp^n hybrids are labeled along dimer or Si–O bonds.

(the latter in parentheses) are listed under each structure. For structures in Figure 1 with one or two absent oxygen atoms, the energies listed correspond to the most stable rearrangement with missing oxygens at another site. The relevant surface structures for one or two oxygen atoms at an independent surface dimer are shown in Figure 4.

In general, those structures which contain the maximum possible number of Si–O bonds are the most stable. Differences in stability between structures with equal numbers of a given type (Si–O, Si–Si, Si–N) are attributed to differences in strain present in each rearrangement geometry. These strains include those of the surface adsorbate ring and lattice strains resulting from subsurface oxygen insertion. While the strain energy is difficult to quantify, we will show that less energetically favored structures are typically associated with larger deviations from the tetrahedral geometry and sp^3 hybridization that are strongly favored for silicon. Using natural bond orbital³⁴ (NBO) analysis to characterize atomic hybridization along each bond axis, we can identify which bonds are most highly strained and how changes in geometry alter the strain energy. We present here some of the more stable rearrangement structures and elucidate the general trends.

To illustrate the strain present in each structure, the contributions of each surface silicon to the dimer bond (or to the Si–O bond, when O is inserted into the dimer) were acquired from NBO analysis. The numbers labeling surface silicon atoms in Figures 1 and 4 are the values of n corresponding to the sp^n hybrid that each dimer Si atom contributes to the bond. Corresponding hybridizations for other atoms are not shown. Most of the strain in these structures is associated with the

surface silicon atoms since these atoms are bonded to both the adsorbate ring and subsurface atoms. In an unstrained system, silicon atoms will have nearly tetrahedral geometry and will contribute an sp^3 hybrid to each bond. When n is substantially larger than 3, the silicon contributes a large p component to the bond, which is a sign of ring strain.

We first examine the migration of a single oxygen from the initial cycloadduct, **I**, into a Si–Si bond to form structures **II** and **IIIa–c**. A precedent for **II** has been observed in the analogous reaction between nitro compounds and disilenes.³¹ In that case the initial 1,3-dipolar cycloadduct rearranges to form a new five-membered ring with one oxygen inserted between the two silicons of the disilene. On the surface, this corresponds to insertion of oxygen in the dimer bond. However, bonds to subsurface atoms prevent the geometry relaxation that occurs in the molecular case, and the resulting structure on the surface is highly strained. This strain is evident in the geometry of **II** where the surface Si atoms are far from tetrahedral. Moreover, NBO analysis shows that the surface Si atoms have a high degree of p -character in their bonds to the inserted oxygen, corresponding (on average) to $sp^{6.3}$ hybrids.

Rearrangement products **IIIa–c** contain a four-membered ring with a Si–Si σ bond. That allows the dimer silicons to have hybridization closer to sp^3 along each bond axis. Whether oxygen is inserted into a back-bond on either side of the adsorbate ring or on an independent dimer has little effect on the energy, making structures **IIIa–c** energetically equivalent to within 1 kcal/mol. The energy listed under structure **IIIc** corresponds to the rearrangement in which one of the oxygens has migrated into the back-bond of a neighboring dimer (Figure 4b). We have also considered the rearrangement in which the oxygen forms a three-membered epoxide ring (Si–O–Si) on the neighboring dimer. Although the epoxide structure (Figure 4a) contains one more Si–Si bond than the structure with the oxygen in the back-bond (Figure 4b) the epoxide is highly strained (sp^{12}) along the dimer bond.

An even more favorable set of structures includes a four-membered ring with oxygen inserted into the dimer bond, **IVa,b** in Figure 1. These structures include one more Si–O bond than **IIIa–c**, but one fewer Si–Si bond. While the Si–Si bond distance (2.51 Å) is similar to that in a normal Si–Si bond, we find (as have several earlier studies on molecular analogues^{35,36}) that the electron density is not consistent with a Si–Si bond. Just as in **II**, a large portion of the energetic gains afforded by oxygen insertion into the dimer bond are compromised by the introduction of ring strain, as evident from the high p -character in the Si contribution to the Si–O bond. In structure **IVb**, the four-membered ring is especially strained, with each surface silicon contributing sp^8 hybrids in the bond to the dimer-inserted oxygen. The presence of oxygen in the back-bond in structure **IVa** partially alleviates this strain, with Si atoms contributing $sp^{4.7}$ and sp^7 hybrids along the analogous bonds.

Yet another set of structures, **Va–c**, include a three-membered ring on the surface. These structures maximize the number of Si–O bonds, but introduce more strain in the surface ring. Like the epoxide, the three-membered Si–N–Si ring is quite strained, as reflected in the high p -character along the Si–Si bond. Just as for **IIIa–c** and **IVa,b**, oxygen inserted in a back-bond partially alleviates the strain present in the surface ring. However, competing with the strains in the surface ring are the strains introduced by oxygen insertion into the back-bond. In addition to the structures shown, other cases in which the oxygens remain in back-bonds adjacent to the surface ring (like **Va**) were considered. There are two possibilities where

oxygens migrate to opposite sides of the dimer: The structure in which the oxygens are “trans” with respect to the dimer bond was found to be slightly less stable than **Va** by 2 kcal/mol; a local minimum was not found for the structure containing oxygens “cis” with respect to the dimer bond, suggesting a very strained geometry. We must also consider cases where one or both oxygens move to an adjacent dimer (structures **Vb** and **Vc**, respectively). Several possible arrangements of oxygen in the adjacent dimer are shown in Figure 4, and the energies for structures **Vb,c** correspond to the most stable arrangement of oxygens in Figure 4. The variation in energy among structures **V** is subtle, involving the back-bond strain in two dimers as well as the adduct ring strain, and a qualitative rationale for the small differences in energy does not appear possible.

In general, the rearrangement of the initial 1,3-dipolar cycloadduct will proceed to structures that increase the number of Si–O bonds and minimize disruption to the tetrahedral lattice geometry. We have not explored kinetic barriers to these rearrangements, and it is possible that only a subset are formed in practice. In particular, while many of the least-strained geometries result from oxidation of neighboring dimers and their back-bonds, there is likely to be a kinetic barrier to oxygen migration.³⁷ Such a barrier would favor oxygen insertion into bonds immediately adjacent to the cycloadduct. If the less stable, two-dimer bridging structure (Figure 2) is formed, the driving force for rearrangement will be even stronger than that for the single-dimer product. Thus, the initial bridging product is less likely to be observed than the single-dimer product.

IV. Final Remarks

Our calculations indicate that nitromethane should nondissociatively chemisorb on the Si(100)- 2×1 surface via a 1,3-dipolar cycloaddition reaction. In fact, we have predicted that this reaction occurs with a wide variety of 1,3-dipoles, as reported elsewhere.³⁸ The cycloaddition proceeds on a concerted reaction path with no significant activation barrier. Though thermodynamically favored over reactants, the 1,3-dipolar cycloadduct is metastable with respect to various rearrangement products. We have not explored the mechanisms or kinetics of these rearrangements.

Standard experiments may be used to probe for the presence (or absence) of structures discussed here. For example, X-ray photoelectron spectroscopy (XPS) may be used to probe for differences in chemical environment resulting from differences in bonding.³⁹ Preliminary experimental measurements indicate that there are three distinct N(1s) binding energies.⁴⁰ Calculated N(1s) orbital energies fall into three distinct groups (separated by 1–2 eV) corresponding to the three general nitrogen bonding environments encountered in our proposed structures, O–N–O, O–N–Si, and Si–N–Si (where it is implicit that nitrogen is also bound to a methyl group). Although N(1s) eigenvalues provide a reasonable first approximation to experimental measurements, they only entail so-called initial-state energies. Quantitative comparisons must account for final-state contributions that include the response of valence electrons to the core “hole”.⁴¹

Infrared (IR) spectroscopy may also be employed to identify the presence of specific structures. We have calculated IR spectra for the structures considered and identified helpful identification signatures. For example, CH stretching modes of rearrangement structures exhibit significant red shifts of, typically 40 cm^{-1} or more with respect to the initial cycloadduct. Similarly, C–N stretches of structures containing Si–N–Si bonds are red-shifted by 200 cm^{-1} or more with respect to the initial cycloadduct. Comparisons to experiment are in progress.

One direct application of nitromethane adsorption on Si(100) is as a model of silicon oxynitride interfaces. The mixture of surface species, with various bonding configurations between oxygen, nitrogen, and silicon, is reminiscent of the possibilities in an oxynitride. Comparison of theory and experiment for nitromethane adsorption should allow calibration of spectroscopic probes that can be used to characterize oxynitride interfaces.

The reaction of nitromethane is simply one example of adsorption of nitro compounds on Si(100). Other nitroalkanes should react in close analogy to nitromethane, since the alkyl chain itself is unreactive. This reaction provides a new route to attaching organic monolayers to Si(100). The likelihood of rearrangements after adsorption means that attachment may occur through a variety of linkages. Thus, the reaction is not likely to be useful in creating highly ordered overlayers. On the other hand, since the optimal spacing between alkyl chains is somewhat larger than the distance between surface sites, there will be an inherent disorder to alkyl overlayers regardless of the attachment chemistry used. That is, in applications where an alkyl monolayer is desired, the possibility of rearrangements is not an obvious shortcoming. Note that attachment of a longer (or branched) alkane offers the possibility of establishing a hydrophobic protecting layer on the surface. Such a layer will certainly be needed if this surface is to be stable outside of ultrahigh vacuum conditions. It remains for experimental work to test the practical value of nitroalkane cycloaddition in surface modification.

Acknowledgment. We wish to thank Stacey Bent, Bob Hamers, Jennifer Hovis, Joe Eng, and Yves Chabal for their interest in testing these predictions, and for discussing preliminary experimental studies of nitromethane adsorption. We also want to acknowledge the support of the National Science Foundation through grants CTS-9724404 and CHE-9971241.

References and Notes

- (1) Padwa, A., Ed. *1,3-Dipolar Cycloaddition Chemistry*; Wiley: New York, 1984.
- (2) Jing, Z.; Whitten, J. L. *Phys. Rev. B* **1992**, *46*, 9544.
- (3) Nachtigall, P.; Jordan, K. D.; Sosa, C. *J. Phys. Chem.* **1993**, *97*, 11666.
- (4) Vittadini, A.; Selloni, A.; Casarin, M. *Phys. Rev. B* **1994**, *49*, 11191.
- (5) Pai, S.; Doren, D. J. *J. Chem. Phys.* **1995**, *103*, 1232.
- (6) Yang, Y. L.; D'Evelyn, M. P. *J. Vac. Sci. Technol. A* **1993**, *11*, 2200.
- (7) Flowers, M. C.; Jonathan, N. B. H.; Morris, A.; Wright, S. *J. Chem. Phys.* **1998**, *108*, 3342.
- (8) Konecny, R.; Doren, D. J. *J. Am. Chem. Soc.* **1997**, *119*, 11098; *Surf. Sci.* **1998**, *417*, 169.
- (9) Teplyakov, A. V.; Kong, M. J.; Kong, S. F. *J. Am. Chem. Soc.* **1997**, *119*, 11000; *J. Chem. Phys.* **1998**, *108*, 4599.
- (10) Konecny, R.; Doren, D. J. *J. Chem. Phys.* **1997**, *106*, 2426.
- (11) Robinson Brown, A.; Doren, D. J. *J. Chem. Phys.* **1998**, *109*, 2442.
- (12) Burdett, J. K. *Chemical Bonding in Solids*; Oxford University Press: New York, 1995.
- (13) Robinson Brown, A.; Doren, D. J. *J. Chem. Phys.* **1999**, *110*, 2643.
- (14) Konecny, R.; Doren, D. J. *J. Phys. Chem. B* **1997**, *101*, 10983.
- (15) Fattal, E.; Radeke, M. R.; Reynolds, G.; Carter, E. A. *J. Phys. Chem B* **1997**, *101*, 8658.
- (16) Widjaja, Y.; Mysinger, M. M.; Musgrave, C. B. *J. Phys. Chem B* **2000**, *104*, 2527.
- (17) Becke, A. D. *J. Chem. Phys.* **1993**, *98*, 1372.
- (18) Lee, C.; Yang, W.; Parr, R. G. *Phys. Rev. B* **1988**, *37*, 785.
- (19) Frisch, M. J., et al.; *Gaussian98*; Gaussian, Inc.: Pittsburgh, PA, 1998.
- (20) Choi, C. H.; Gordon, M. S. *J. Am. Chem. Soc.* **1999**, *121*, 11311.
- (21) Fitzgerald, D. R.; Doren, D. J. *J. Am. Chem. Soc.*, submitted for publication.
- (22) Föraker, A. C.; Doren, D. J., manuscript in preparation.
- (23) Liu, J.; Niwayama, S.; You, Y.; Houk, K. N. *J. Org. Chem.* **1998**, *63*, 1064.
- (24) Klicic, J. J.; Friesner, R. A. *J. Phys. Chem.* **1999**, *103*, 1276.
- (25) Su, M.-D.; Liao, H.-Y.; Chung, W.-S.; Chu, S.-Y. *J. Org. Chem.* **1999**, *64*, 6710.
- (26) Nguyen, M. T.; Chandra, A. K.; Sakai, S.; Morokuma, K. *J. Org. Chem.* **1999**, *64*, 65.
- (27) Branchadell, V.; Muray, E.; Oliva, A.; Ortuño, R. M.; Rodriguez-Garcia, C. *J. Phys. Chem.* **1998**, *102*, 10106.
- (28) Barone, V.; Arnaud, R. *J. Chem. Phys.* **1997**, *106*, 8727.
- (29) Stefanov, B. B.; Gurevich, A. B.; Weldon, M. K.; Raghavachari, K.; Chabal, Y. J. *Phys. Rev. Lett.* **1998**, *81*, 3908.
- (30) Wilson, A. J. C. Ed.; *International Tables for Crystallography*; Kluwer: Dordrecht, 1995.
- (31) Gillete, G. R.; Maxka, J.; West, R. *Angew. Chem., Int. Ed. Engl.* **1989**, *28*, 54.
- (32) Houk, K. N.; Gonzalez, J.; Li, Y. *Acc. Chem. Res.* **1995**, *28*, 81.
- (33) Emsley, J. *The Elements*; Clarendon Press: Oxford, UK, 1993.
- (34) Glendening, E. D.; Badenhoop, J. K.; Reed, A. E.; Carpenter, J. E.; Weinhold, F. *NBO 4.0*; Theoretical Chemistry Institute, University of Wisconsin: Madison, WI, 1996.
- (35) O'Keefe, M.; Gibbs, G. V. *J. Phys. Chem.* **1985**, *89*, 4574.
- (36) Gordon, M. S.; Packwood, T. J.; Carroll, M. T.; Boatz, J. *J. Phys. Chem.* **1991**, *95*, 4332.
- (37) Weldon, M. K.; Stefanov, B. B.; Raghavachari, K.; Chabal, Y. J. *Phys. Rev. Lett.* **1997**, *79*, 2851.
- (38) Barriocanal, J. A.; Doren, D. J. *J. Vac. Sci. Technol. A* **2000**, *18*, in press.
- (39) Rignase, G. M.; Pasquarello, A.; Charlier, J. C.; Gonze, X.; Car, R. *Phys. Rev. Lett.* **1997**, *79*, 5174.
- (40) Chabal, Y. J.; Eng, J., private communication.
- (41) Pehlke, E.; Scheffler, M. *Phys. Rev. Lett.* **1993**, *71*, 2338.